Molecular Crystals and Liquid Crystals

Publication details, including instructions for authors and subscription information:
http://www.tandfonline.com/loi/gmcl20

Numerical Simulation of a Twisted Nematic Cell Constructed From Micropatterned Substrates

T. J. Atherton [a] & J. R. Sambles [a]

[a] Thin Film Photonics Group, School of Physics, University of Exeter, Stocker Road, Exeter, England

Version of record first published: 22 Sep 2010

To cite this article: T. J. Atherton & J. R. Sambles (2007): Numerical Simulation of a Twisted Nematic Cell Constructed From Micropatterned Substrates, Molecular Crystals and Liquid Crystals, 475:1, 3-11

To link to this article: http://dx.doi.org/10.1080/15421400701732308

Mol. Cryst. Liq. Cryst., Vol. 475, pp. 3–11, 2007

ISSN: 1542-1406 print/1563-5287 online
DOI: 10.1080/15421400701732308

Taylor & Francis
Taylor & Francis Group

Numerical Simulation of a Twisted Nematic Cell Constructed From Micropatterned Substrates

T. J. Atherton
J. R. Sambles
Thin Film Photonics Group, School of Physics, University of Exeter, Stocker Road, Exeter, England

A numerical model of the director field of a nematic in contact with a micropatterned surface has been developed. For a surface that consists of alternate homeotropic and planar stripes, it is found that differences between the elastic constants (of similar magnitude to those measured in commonly used materials) lead to considerable variation in the surface pretilt promoted by a micropatterned surface. It is furthermore shown that the director configuration adopted by a nematic in a Twisted Nematic (TN) cell constructed from orthogonally micropatterned substrates is sensitive to small changes in the elastic constants and the response to an applied field is calculated.

Keywords: elastic anisotropy; micropatterned surfaces; nematic; TN cell

I. INTRODUCTION

Surfaces patterned on the nanometre and micron scale are interesting as a possible means of creating bistable liquid crystal displays [1]. A variety of techniques exist to fabricate patterned surfaces: development of a photoalignment polymer film with appropriate masks [2]; microcontact printing of Self-Assembled Monolayers (SAMS) of functionalized alkenethiols [3–6]; AFM scribing of a surface to create nanoscale patterns [1,7,8]. Typically, a patterned surface incorporates certain regions that promote homeotropic alignment and other regions that promote planar alignment, or planar regions with different easy

The authors would like to acknowledge the EPSRC and Sharp Laboratories of Europe for financial support and to thank Dr N. J. Smith of Sharp for helpful discussion.

Address correspondence to T. J. Atherton, Thin Film Photonics Group, School of Physics, University of Exeter, Stocker Road, Exeter, England, Ex4 4QL, UK. E-mail: t.j.atherton@ex.ac.uk

axes. Immediately above such a surface the nematic director field $\hat{\mathbf{n}}$ is highly distorted; away from the surface the nematic adopts a uniform bulk orientation that depends on the relative area of the different regions: it is possible therefore to design a surface that promotes any desired orientation in the bulk nematic.

One pattern that has been studied theoretically is a periodic array of alternate planar and homeotropic stripes. For a nematic with equal elastic constants where the director is confined to a single plane, Barbero *et al.* derived a Fourier series solution for the director profile and found the bulk orientation as a function of pretilt angles and surface anchoring strength [9]. Okano *et al.* found an analogous solution using the technique of conformal mapping [10].

Kondrat *et al*. showed that if either the planar or homeotropic set of stripes was much narrower than the other set, then the nematic might adopt a spatially uniform configuration rather than the distorted configuration [11]. Finally and most recently, we extended [12] Barbero *et al.'s* approach to consider the situation where $K_2 \neq K_1 = K_3$ (K_1, K_2 and K_3 are the elastic constants associated with splay, twist and bend distortions respectively). We showed that if $K_2 < K_1$, a nematic in contact with such a surface has lower elastic energy when the component of the director in the plane of the substrate lies along the length of the stripes. If the planar stripes are prepared so that the easy axis is perpendicular to the elastically preferred direction, there exists the possibility that the director might "twist out" so as to lie perpendicular to the easy axis if the azimuthal anchoring strength of the planar stripes is sufficiently low relative to the elastic constants.

Analytical solutions for the director field exist only when the director field is confined to a single plane and where at least the splay and bend elastic constants are equal. In this article a numerical model of the director field is developed that is not subject to these limitations: this model is used to determine the effect of splay-bend anisotropy on the uniform bulk orientation promoted by the surface. A Twisted Nematic (TN) device constructed from two orthogonally patterned substrates is also modelled and the behaviour contrasted with a conventional TN device.

II. NUMERICAL MODEL

Adopting the coordinate system illustrated in Figure 1, in which the x axis lies orthogonal to the length of the stripes and the z axis is perpendicular to the surface, the director field $\hat{\mathbf{n}}$ must be a function of x and z alone. The director may be written in cartesian component

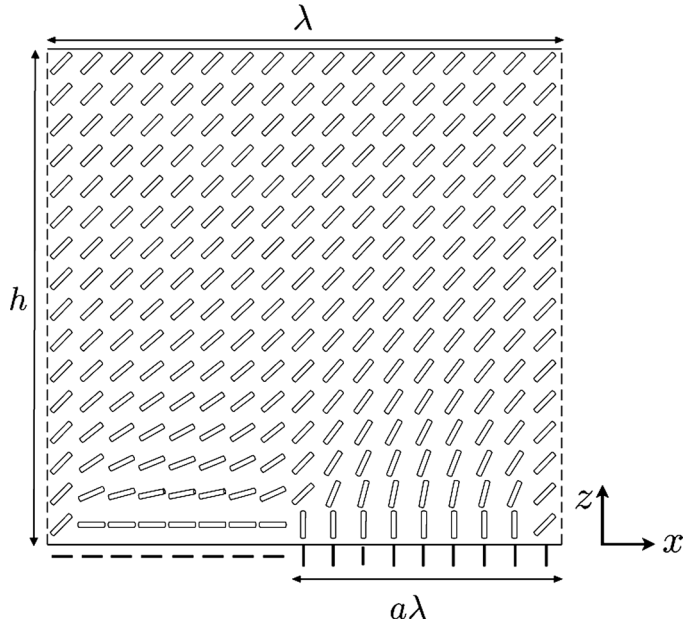

FIGURE 1 Schematic of the director field for a nematic in contact with an array of period λ of planar and homeotropic stripes with mark-space ratio a. The computational domain extends to a height h above the surface.

form

$$\hat{\mathbf{n}}(x,z) = [n_x(x,z), n_y(x,z), n_z(x,z)]; \tag{1}$$

and is subject to the constraint $n_x^2 + n_y^2 + n_z^2 = 1$. We adopt the cartesian representation in preference to the polar representation because with the latter representation if the director is homeotropic then the azimuthal Euler-Lagrange equation is ill-posed (in the sense that the azimuthal component ϕ is multivalued). The actual director configuration is that which minimizes the well-known free energy [13]

$$F = \frac{1}{2}\int [K_1(\nabla\cdot\hat{\mathbf{n}})^2 + K_2(\hat{\mathbf{n}}\cdot\nabla\times\hat{\mathbf{n}})^2 + K_3|\hat{\mathbf{n}}\times\nabla\times\hat{\mathbf{n}}|^2 - \epsilon_0\epsilon_\perp(\nabla U)^2 - \epsilon_0\Delta\epsilon(\hat{\mathbf{n}}\cdot\nabla U)^2]dV \tag{2}$$

where $\epsilon_\perp$ is the dielectric permittivity of the liquid crystal associated with any direction orthogonal to the director, $\Delta\epsilon$ is the dielectric anisotropy and *U(x, z)* is the electric potential field. In this article

we restrict our attention to the situation where the director is fixed at a boundary, and so surface terms are omitted from (2). In order to ensure the modulus of the director is unity at all points in space, (2) must be supplemented by an auxiliary functional,

$$F' = F + \int \lambda(x, z)(n_x^2 + n_y^2 + n_z^2 - 1)dV, \tag{3}$$

with an associated Lagrange multiplier field $\lambda(x,z)$. The director field that minimizes (3) is found by solving the coupled Euler-Lagrange equations for each component

$$\mathcal{E}_{n_i} = \frac{\partial F'}{\partial n_i} - \nabla \cdot \frac{\partial F'}{\partial \nabla n_i} = 0, \quad i \in \{x, y, z\}. \tag{4}$$

and the Maxwell equation for the scalar potential

$$\nabla \cdot (\varepsilon \nabla U) = \nabla \cdot [\epsilon_\perp \nabla U + \Delta\epsilon(\hat{\mathbf{n}} \cdot \nabla U)\hat{\mathbf{n}}] = 0 \tag{5}$$

where ε is the dielectric tensor.

In the one constant approximation (i.e., setting $K = K_1 = K_2 = K_3$), the elastic terms in (2) reduce to

$$f_{el} = K(\nabla \cdot \hat{\mathbf{n}})^2 dV. \tag{6}$$

The Euler-Lagrange equations for the director components in the absence of an applied electric field each reduce to the Laplace equation which may be solved by any of a variety of well-known techniques including conformal mapping and Fourier series. We recently showed that for a nematic with an anisotropic twist constant (i.e., $K_2 \neq K_1 = K_3$) the Euler-Lagrange equation may be similarly reduced to Laplace's equation if the z coordinate is scaled appropriately.

In the general case, however, (4) and (5) must be solved numerically. The computational domain is discretized onto a $N_x \times N_z$ rectangular mesh with a unit cell of width $\delta x = 1/(N_x - 1)$ and height $\delta z = 1/(N_z - 1)$ and where the field variables n_x, n_y, n_z and U are stored at the corners of the rectangles. The Euler-Lagrange equations may then be discretized using cell-centred finite differences

$$\begin{aligned} \nabla q &\to \left(\frac{q_{i+1,j} - q_{i-1,j}}{2\delta x}, \frac{q_{i,j+1} - q_{i,j+1}}{2\delta z}\right) \\ \nabla^2 q &\to \frac{q_{i+1,j} + q_{i-1,j} - 2q_{i,j}}{\delta x^2} + \frac{q_{i,j+1} + q_{i,j-1} - 2q_{i,j}}{\delta z^2} \end{aligned} \tag{7}$$

$$\frac{\partial q}{\partial x \partial z} \to \frac{(q_{i+1,j} - q_{i-1,j})(q_{i,j+1} - q_{i,j-1})}{4\delta x \delta z} \tag{8}$$

where the $q_{i,j}$ represents the value of a field variable or functional q evaluated at coordinates$(x, z) = (i\delta x, j\delta z)$. Along the bottom, Dirichlet conditions are imposed to set the director components at each stripe and periodic boundary conditions are imposed at the left and right hand sides. The boundary condition $\nabla q = 0$ is imposed at the top edge for the director components and U is set to the value of an applied voltage.

Discretization yields $(N_x - 1) \times N_z \times 4$ nonlinear equations f_i and field variables q_i which may be solved by taking Newton steps [14]

$$\mathbf{q}^{t+1} = \mathbf{q}^t + J^{-1}F(\mathbf{q}^t) \tag{9}$$

until convergence ($J = \partial f_i/\partial q_i$ is the Jacobian matrix for the set of nonlinear equations). We stagger the update of the director components and scalar potential values for numerical stability: we first compute updated scalar potential values $V_{i,j}$ via (9) from the Maxwell equations holding director components values constant and then compute updated director components $(n_x, n_y, n_z)_{i,j}$ holding the scalar potential values constant; during the latter part we first compute the Newton step for the director components at each mesh point and then solve for each Lagrange multiplier to maintain normalization.

To simulate a complete cell, the Euler-Lagrange equations must in general be solved in all 3 spatial dimensions. If, however, the cell thickness is sufficiently large in the sense that $d \gg \lambda$, the director field in the centre of the cell depends on the z coordinate alone. The cell may therefore be divided into three regions: near each of the substrates the director is a function of the coordinate perpendicular to the length of the stripes and z and so the director field is solved in these two regions in 2 dimensions as described previously; in the centre of the cell a 1 dimensional solver is used. Boundary conditions at the connecting interfaces are imposed so that the field variables and their derivatives with respect to z are continuous.

III. SIMULATION AND DISCUSSION

We first simulated a region of nematic in contact with a single patterned substrate (Fig. 2) to determine the effective pretilt—the orientation of the director far above the surface—as a function of the homeotropic-planar "mark-space ratio" a. The height h of the computational domain (Fig. 1) was successively extended until the pretilt value obtained for each a was unchanged. The calculation was repeated for different K_3. In typical nematic compounds K_3 is greater than K_1; the calculation was performed using the ratio for E7

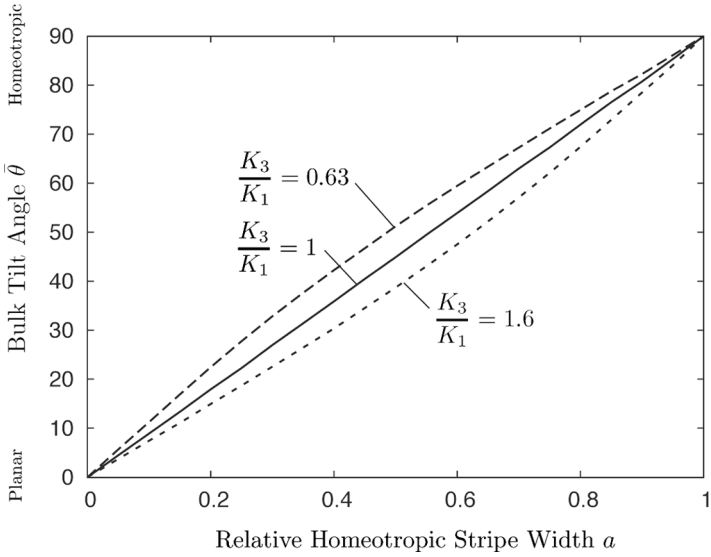

FIGURE 2 Equilibrium bulk tilt angle θ where $n_z = \sin\theta$ as a function of relative homeotropic stripe width a with rigid anchoring for three values of K_3/K_1.

$K_3/K_1 = 1.6$ [15] and again with the inverse. The effective pretilt tends towards homeotropic if $K_3 < K_1$ and towards planar if $K_3 > K_1$. The twist elastic constant does not affect the effective pretilt when the director is perpendicular to the length of stripes as the twist term in the free energy (2) is zero [12].

We then simulated a twisted nematic cell constructed from two micropatterned substrates where the alignment on the planar stripes was fixed to be along the length of the stripes.

The director profiles obtained (Fig. 3) are plotted using the polar representation

$$\hat{\mathbf{n}} = (\cos\theta\cos\phi, \cos\theta\sin\phi, \sin\theta) \tag{10}$$

computed from the cartesian components. They differ significantly for those for a conventional Freedericksz twist cell [16] (where the surface pretilt is 0°) in that the director tends toward homeotropic in the centre of the cell due to the large effective pretilt at the surfaces. The polar profile also varies considerably (Fig. 3)—the central tilt changes by up to 20°—with what amounts to natural differences in elastic constants between physical liquid crystal materials. As in the semi-infinite case, $K_3 < K_1$ favours homeotropic alignment

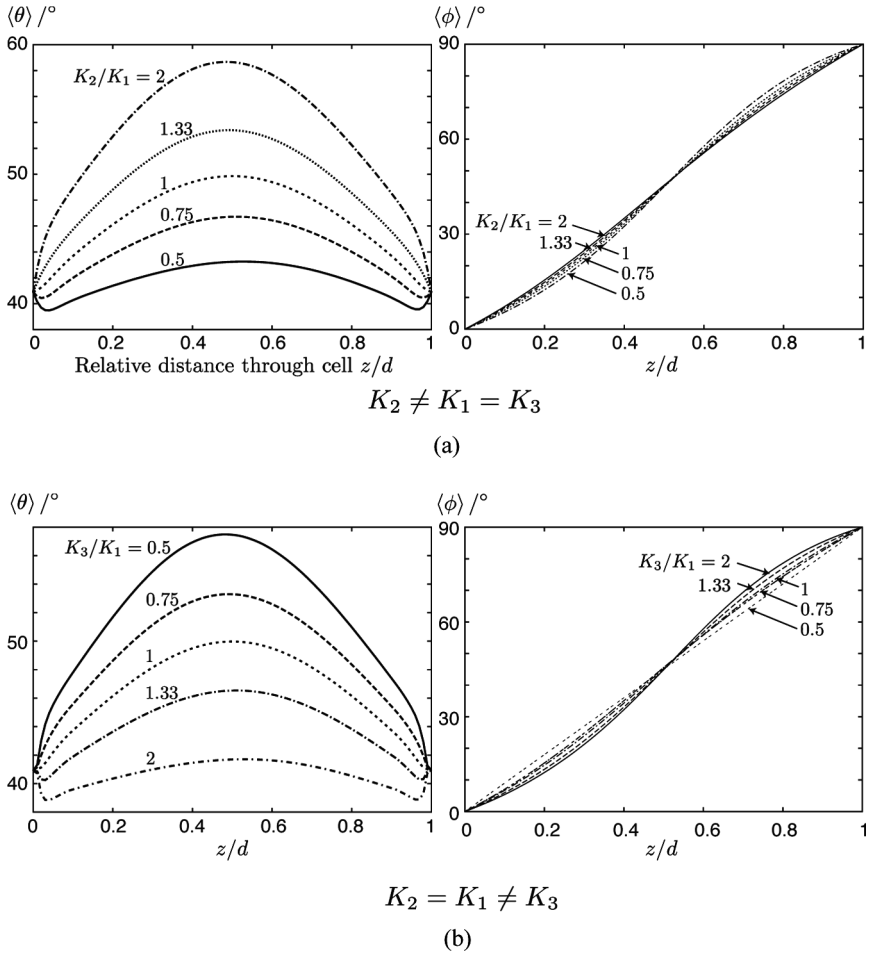

FIGURE 3 Director profiles for a simulated cell of 20 μm thickness with identically patterned substrates of 2 μm period. Director values are shown averaged over the x and y coordinates.

and $K_3 > K_1$ favours planar alignment; the situation is reversed for K_2: $K_2 > K_1$ favours homeotropic alignment and $K_2 < K1$ favours planar alignment.

Finally, we computed the response of the director field to an applied voltage (Fig. 4) with $\epsilon_\perp = 1$, $\Delta\epsilon = 1$ and $K_1 = K_2 = K_3 = 1 \times 10^{-11}\,\mathrm{Jm}^{-2}$. A conventional TN cell with $\theta = 0$ at each surface only switches above a threshhold voltage which is, in the 1-constant

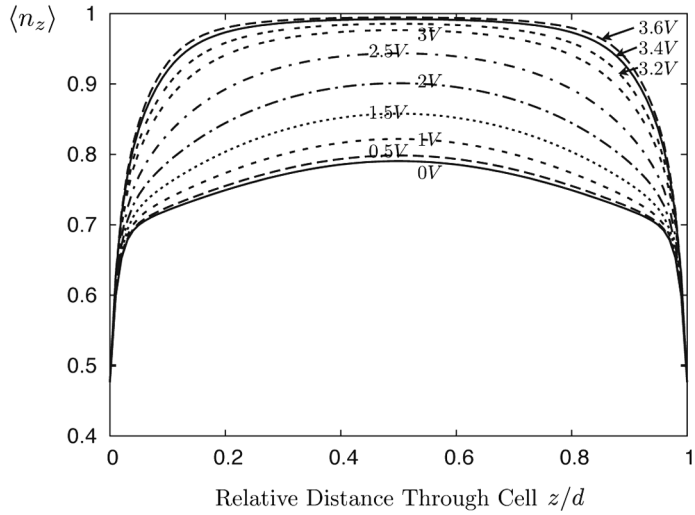

FIGURE 4 Director profile, averaged over the x and y coordinates, for a simulated cell of 20 μm thickness with identically patterned substrates of 2 μm period at several values of applied voltage.

approximation [16],

$$V_C = \sqrt{\frac{K}{\epsilon_0 \Delta\epsilon}} \tag{11}$$

For the values used here $V_C \approx 3.3\,\mathrm{V}$. The micropatterned TN cell simulated has, in contrast to the conventional TN cell, virtually switched at $V = V_C$.

IV. CONCLUSIONS

We have simulated a twisted nematic (TN) cell constructed from two micropatterned surfaces. Our solver splits the cell into two 2-dimensional regions adjacent to either substrate and a 1-dimensional region in the cell centre. This approach is significantly more efficient than solving the full 3-dimensional Euler-Lagrange equations, although that would be necessary if the cell thickness is close to the period of the patterning.

Micropatterned surfaces offer the possibility of constructing TN cells with arbitrary preferred surface alignment orientations, in

particular polar angles around 45° which are very difficult to achieve with conventional uniform substrates. We have shown that the resulting cells offer essentially threshhold-less switching and require much lower voltages than conventional TN cells to switch the cell. Furthermore, the director profile in the cell depends very strongly on the elastic constants; such cells may potentially be used experimentally to measure ratios of elastic constants although there remains the problem of covariance between the two ratios K_2/K_1 and K_3/K_1.

REFERENCES

[1] Kim, J. H., Yoneya, M., & Yokoyama, H. (2002). *Nature*, *420*, 159.
[2] Schadt, M., Schmitt, K., Kozinkov, V., & Chigrinov, V. (1992). *Japanese Journal of Applied Physics*, *21*, 2155.
[3] Kumar A. & Whitesides, G. (1993). *Appl. Phys. Lett.*, *63*, 2002.
[4] Gupta, V. & Abbott, N. (1997). *Science*, *276*, 1533.
[5] Drawhorn, R. & Abbott, N. (1995). *J. Phys. Chem.*, *99*, 16511.
[6] Cheng, Y., Batchelder, D., Evans, S., Henderson, J., Lydon, J., & Ogier, S. (2000). *Liq. Cryst.*, *27*, 1267.
[7] Kim, J., Yoneya, J., Yamamoto, J., & Yokoyama, H. (2001). *Appl. Phys. Lett.*, *78*, 3055.
[8] Zhang, B., Lee, F., Tsui, O., & Sheng, P. (2003). *Phys. Rev. Lett.*, *91*, 215501.
[9] Barbero, G., Beica, T., Alexe-Ionescu, A. L., & Moldovan, R. (1992). *J. Phys. II France*, *2*, 2011.
[10] Okano, K., Kitahara, K., & Ushizawa, E. (1994). *Jpn. J. Appl. Phys.*, *33*, 6262.
[11] Kondrat, S., Poniewierski, A., & Harnau, L. (2003). *Eur. Phys. J. E.*, *10*, 163.
[12] Atherton T. J. & Sambles, J. R. (2006). *Phys. Rev. E*, *74*, 022701.
[13] Chandrasekhar, S. (1992). *Liquid Crystals*, 2nd ed. Cambridge University Press.
[14] Press, W. H., Teukolsky, S. A., Vetterling, W. T., & Flanner, B. P. (1988). *Numerical Recipes in C: The Art of Scientific Computing*, Cambridge University Press: Cambridge, 379–393
[15] *E7 data sheet, Merck KGaA*.
[16] Stewart, I. W. (2004). *The Static and Dynamic Continuum Theory of Liquid Crystals*, Taylor & Francis: London, 57–100.